

Modelling of the magnetic accretion flow in HU Aquarii

Claus Heerlein^{1,2,3}, Keith Horne¹ and Axel D. Schwope²

¹ *University of St. Andrews, School of Physics and Astronomy, North Haugh, St. Andrews, Fife KY16 9SS, Scotland*

² *Astrophysikalisches Institut Potsdam, An der Sternwarte 16, D-14482 Potsdam, Germany*

³ *Institut für Theoretische Physik II, Universität Erlangen-Nürnberg, Staudstr. 7, D-91058 Erlangen, Germany*
e-mail: claus.heerlein@theorie2.physik.uni-erlangen.de

submitted: 1998 May 5, re-submitted: 1998 September 18

ABSTRACT

We present a magnetic stripping model for AM Her type objects. Our model is based on an equilibrium condition between ram pressure and magnetic pressure in a stiff dipolar magnetic field. We investigate the detailed geometry of the stripping process, most of which can be tackled analytically. By involving additional numerical calculations, the model allows the prediction of phase-resolved spectra and Doppler tomograms. The emission line features from the companion star, the horizontal stream and the accretion curtain are identified with the emission line components found by Gaussian fitting to observational data of HU Aqr in its high accretion state. Given the simplicity of the model, its agreement with the observation is remarkably good and enables us to derive a number of physical quantities such as stellar masses and radii, total mass accretion rate, bulk temperature, and coupling density.

Key words: accretion - magnetic cataclysmic variables - AM Her objects - modelling - stars: individual: HU Aqr

1 INTRODUCTION

Magnetic cataclysmic variables (MCVs) are binary systems consisting of a late-type near main sequence secondary star and a magnetic white dwarf primary. Matter lost by Roche lobe overflow from the secondary star interacts with the strong magnetic field of the white dwarf before being finally accreted. These systems are ideal laboratories for studying the interaction of supersonic gas streams with strong magnetic fields.

In an AM Her object, or “polar”, the magnetic field of the synchronously rotating white dwarf is sufficiently strong to prevent the formation of an accretion disk. A relatively bright representative of this class is the eclipsing polar HU Aqr with an orbital period of $P = 0.^d08682$. It has been under intensive study (e.g. Glenn et al. 1994, Hakala 1995, Schwartz et al. 1995) since its identification in 1992 (Hakala et al. 1993, Schwope et al. 1993). The strength and orientation of the primary’s dipolar magnetic field has been determined with fair precision from cyclotron harmonics observed in low resolution spectra, from polarisation measurements, and from the X-ray light curve; it was found for the magnetic field strength and the position of the accretion spot, respectively, $B_s \approx 35\text{MG}$, $\varphi_s \approx 40^\circ$, $\vartheta_s \approx 26^\circ$. The mass ratio and inclination of the system remain somewhat more uncertain ($Q := M_{\text{wd}}/M_{\text{rd}} \in [2.5, 5.7]$, $i \in [81^\circ, 90^\circ]$), but the eclipse phase width $\Delta\phi = 0.0763$ however imposes a tight relationship between Q and i . Doppler maps gener-

ated from high resolution trailed spectra by Schwope et al. (1997a) clearly show that the illuminated face of the secondary star’s Roche lobe and the accretion stream in the orbital plane are the dominant emission-line features of the high accretion state. The observed structure of the horizontal stream indicates that the stream initially follows the ballistic trajectory and we are therefore dealing with the situation described by Liebert & Stockman (1985), in which thermal pressure dominates magnetic pressure at the inner Lagrangian point L_1 . Recent observations suggest that this no longer holds for the reduced accretion state, when the density of the stream is significantly lower (Schwope et al. 1997b). Then, as proposed by Mukai (1988), the flow may couple directly to the magnetosphere at the L_1 -point as assumed in early AM Her models (e.g. Schneider & Young (1980) for VV Pup).

In this article we develop a simple but predictive model for phase-resolved emission line profiles and Doppler tomograms of MCV’s. We test this model on observations of HU Aqr in its high accretion state. The accretion stream starts at the inner Lagrangian point L_1 from the Roche lobe of the secondary star as shown in Figure 1. The initial part of the stream, not yet affected by the magnetic field, is confined to the orbital plane and is hence called the horizontal stream. In our calculations it is assumed to have a Gaussian density profile that is however truncated when the density drops below a critical value below which the matter couples to the magnetosphere. This stripping threshold, displayed

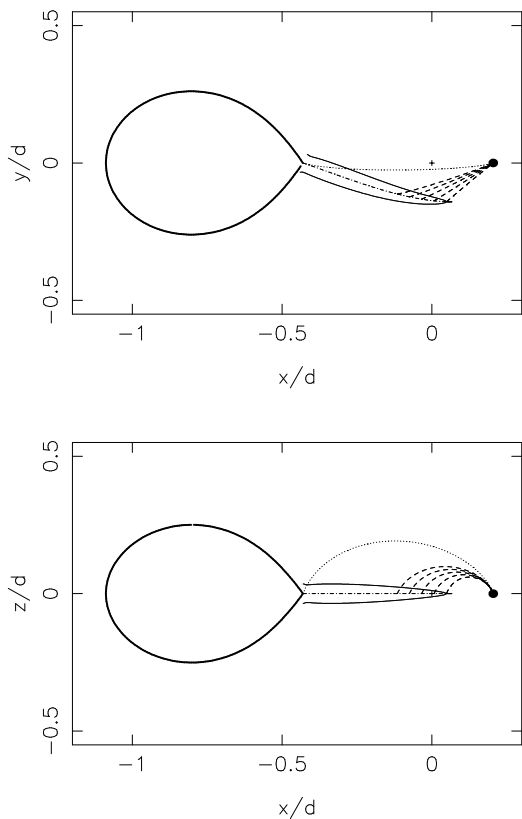


Figure 1. Sketch of the HU Aqr system projected on the x-y-plane (top) and x-z-plane (bottom); see text for details.

by the solid lines around the stream centre in Figure 1, is defined by the ram pressure in the stream dropping below the magnetic pressure of a stiff dipole field. The stripped material, as it leaves the orbital plane, forms a two-dimensional accretion curtain and glides along the field lines until it is finally accreted on the white dwarf’s surface. Even though magnetic stripping occurs virtually over the whole length of the horizontal stream, most of the matter is stripped near the end of the horizontal stream, as indicated by the dashed lines in Figure 1. The curtain trajectory passing through the end point of the horizontal stream has been named vertical stream in the literature. The dotted line marks the trajectory of matter that is stripped right at the L_1 -point (see below).

X-ray radiation from the accretion region excites line emission from the companion star surface and the accretion stream. The line emission from the secondary star was found to be optically thick in our initial study (Schwope et al. 1997a), whereas for the emission from the horizontal stream and the curtain the situation is less obvious and we are here comparing the limiting cases of optically thin and thick radiation reprocessing.

We first focus in Section 2 on the horizontal stream and derive the stripping rate with which matter is removed from it by the magnetic field. In Section 3 we investigate the geometry of the accretion curtain in which the matter prop-

agates through the magnetosphere. Our model provides the velocity vector and densities at each point of the flow, enabling us to model phase-resolved spectra and Doppler maps in Section 4, which are fitted to observations of HU Aqr in Section 5. This allows us to derive the physical quantities of the system such as stellar masses and radii, total mass accretion rate, bulk temperature, and coupling density. Finally in Section 6 we discuss the discrepancies of model and observation and propose further improvements.

2 MAGNETIC STRIPPING

2.1 The horizontal stream

As suggested by the high-state observations, the stream is not strongly affected by the magnetic field as it passes the inner Lagrangian point L_1 . This situation invites use of the semi-analytical solution for an inviscid isothermal flow in a Roche potential given by Lubow & Shu (1975, 1976) with additional corrections for the magnetic influence. First the applicability of the Lubow-Shu-model on AM Her stars deserves some discussion: (a) The stream and secondary star are heated by ionising radiation from the accretion region. The diminished line emission of the secondary’s leading side implies considerable shielding by the accretion curtain (Schwope 1997a), which must therefore have a high optical depth for the ionising radiation. The column density there is even lower than in the horizontal stream, where we consequently also expect a high optical depth. This confines the irradiative heating to the skin layers and causes a highly inhomogeneous temperature distribution over the stream. We assume that the bulk of matter in the stream centre remains at a constant temperature and the overall behaviour of the stream is not much affected by the hot surface layer. We also neglect the impact of radiation pressure on the stream. (b) In the region where the magnetic pressure already overcomes the thermal pressure but not yet the ram pressure, which is the case for almost the whole stream apart from a very thin shell around the L_1 -point, instabilities shatter the stream to small blobs (Liebert & Stockman 1985). We assume that the mean density on a scale comparable to the stream width is still described by a simple Gaussian profile as originally proposed by Lubow & Shu. In the Reynolds averaged sense we treat the ensemble of gas blobs as a quasi-steady flow and assume a vanishing eddy-viscosity therein. (c) Further downstream magnetic stripping erodes the stream from the outside. This violates the assumption of a Gaussian density distribution and might also affect the temperature structure. Even though the stream motion is highly supersonic the internal gas pressure is important in the transverse directions of the flow. Our model however assumes for simplicity that the magnetic pressure exerted on the surface of the stream is equal to the pressure that the stripped layers would have exerted, so that the kinematic behaviour of the core is not affected by the missing envelope.

Following the suggestion of Lubow & Shu (1975) we formulate the problem in dimensionless units of length, time and mass:

$$1[L] = d, \quad 1[T] = \Omega^{-1}, \quad 1[M] = \dot{M}\Omega^{-1}, \quad (1)$$

where d is the orbital separation of the system, $P = 2\pi/\Omega$ its rotation period, and \dot{M} the total mass accretion rate.

Also from Lubow & Shu (1975) we adopt the treatment as a perturbation analysis in a small parameter ϵ , which is the isothermal sound speed $\sqrt{kT/m}$ in the stream for a temperature T and a mean molecular weight m in above units given by Equation (1). Under the assumption of an isothermal flow the perturbation parameter ϵ is constant over the whole accretion stream. For the orbital period of the HU Aqr system we have in case of a pure hydrogen gas $\epsilon = 0.011(T/10^4 K)^{1/2}(d/10^9 m)^{-1}$.

Initially we consider a stream without a magnetic field. We use the natural coordinate system of the horizontal stream where s measures the distance from the L_1 -point along the stream centre and the pair (n, z) represents the distances from the stream centre parallel and perpendicular to the orbital plane. Lubow & Shu (1975, 1976) propose that the density in the horizontal stream has a Gaussian distribution around the ballistic trajectory, i.e.

$$\rho(s, n, z) = \rho_0(s) \exp\left(-\frac{1}{2\epsilon^2}(\gamma n^2 + \chi z^2)\right), \quad (2)$$

where the characteristic horizontal and vertical widths $1/\sqrt{\gamma}$ and $1/\sqrt{\chi}$, respectively, are functions of s only and can be found from an initial value problem as the solution of a closed set of non-linear singular differential equations, in which the mass fraction μ appears as a parameter; the mass fraction is defined as the white dwarf mass over the total mass: $\mu := M_{\text{wd}}/(M_{\text{wd}} + M_{\text{rd}})$. A proper numerical integration of these equations requires asymptotic analysis near the singular point L_1 (see Appendix A). With u_{s0} as the s -component of the stream velocity in the centre we have in lowest order of ϵ

$$\rho_0(s) = \frac{\sqrt{\gamma\chi}}{2\pi\epsilon^2 u_{s0}}, \quad (3)$$

since we have normalised our equations to the total mass flow, i.e. $\int \rho u_{s0} dn dz = 1$ and the local stream velocity u_s can be approximated by the central velocity u_{s0} in lowest order of ϵ .

2.2 The stripping process

The ram pressure of the stream orthogonal to the magnetic field can be written as

$$\begin{aligned} p_{\text{ram}} &= \frac{1}{2} \rho u_{s0}^2 \sin^2 \varpi = \\ &= \frac{\sqrt{\gamma\chi} u_{s0} \sin^2 \varpi}{4\pi\epsilon^2} \exp\left(-\frac{1}{2\epsilon^2}(\gamma n^2 + \chi z^2)\right), \end{aligned} \quad (4)$$

where ϖ is the stripping angle between stream motion and the magnetic field. Further the thermal pressure of the gas is given by

$$p_{\text{th}} = \epsilon^2 \rho = \frac{\sqrt{\gamma\chi}}{2\pi u_{s0}} \exp\left(-\frac{1}{2\epsilon^2}(\gamma n^2 + \chi z^2)\right). \quad (5)$$

We now compare the total gas pressure $p_{\text{th}} + p_{\text{ram}}$ in the stream with the local magnetic pressure $p_{\text{mag}} = B^2/(8\pi)$. We assume then that the stripping threshold is given by $p_{\text{th}} + p_{\text{ram}} = p_{\text{mag}}$. Since we are considering the stripping process at large distances from the dipole source we approximate the local B by the magnetic field B_0 at the stream centre with an error of order ϵ . Using Equation (4) & (5) we find that the critical surface is a centred ellipse with the principal

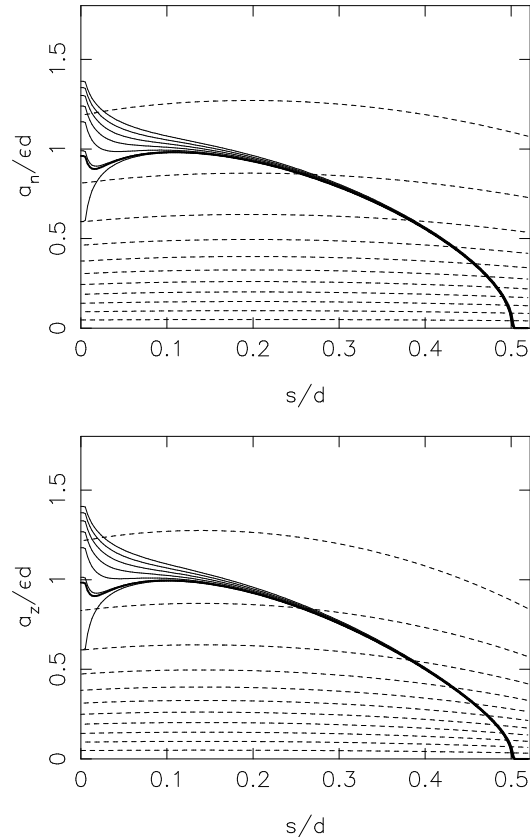


Figure 2. Stripping threshold (solid lines) in n and z direction, respectively for $\epsilon = 0$ to 0.24 in steps of 0.04 ; the remaining parameters are as in Table 1. Superimposed (dashed lines) are stream lines for the 10% to 90% (in steps of 10%), 97.5% and 99.9% percentiles.

axes a_n and a_z aligned to the coordinate axes perpendicular to the direction of propagation:

$$a_n = \epsilon \sqrt{\frac{2\sigma}{\gamma}}, \quad a_z = \epsilon \sqrt{\frac{2\sigma}{\chi}} \quad (6)$$

with

$$\sigma := \ln\left(\frac{2\sqrt{\gamma\chi}(u_{s0}^2 \sin^2 \varpi + 2\epsilon^2)}{\epsilon^2 B_0^2 u_{s0}}\right). \quad (7)$$

For numerical calculations we assume a dipole field

$$\mathbf{B} = \frac{3\mathbf{r}_{\text{wd}}(\mathbf{r}_{\text{wd}} \cdot \mathcal{M}) - r_{\text{wd}}^2 \mathcal{M}}{r_{\text{wd}}^5}, \quad (8)$$

with r_{wd} the distance from the white dwarf centre and \mathcal{M} the magnetic moment. Figure 2 shows numerically calculated streamlines and stripping surfaces for the geometry of HU Aqr. Minima in a_n and a_z occur immediately after the L_1 point for $\epsilon \lesssim 0.08$, i.e. for a cold stream. They arise because the thermal pressure decreases due to the dilution caused by the acceleration of the stream before the ram pressure increases enough to take over the pressure balance with p_{mag} that provides our stripping condition. The locations of the minima are close to the equilibrium point between thermal pressure and magnetic pressure, downstream

from which Liebert & Stockman (1985) postulate shattering of the stream into fine blobs. The presence of minima in the stripping thresholds suggests a ‘magnetic nozzle’ at the beginning of the horizontal stream, however one should be cautious with that interpretation since the diamagnetism of the secondary star, and possibly its intrinsic magnetic field, induce in the vicinity of L_1 a large distortion of the ideal dipole field assumed in our model. The observed trailed spectra of HU Aqr show no evidence for a manifest stripping directly at the L_1 -point. Cropper (1986) however concludes from polarisation measurements in ST LMi that a two-spot accretion is the best fit to his data, so stripping directly at the L_1 -point may occur in other AM Her objects. Since we can fit the parameter ϵ only very indirectly (c.f. Section 5) it is very reassuring that towards the end of the horizontal stream, where we expect the largest proportion of the magnetic stripping to occur (c.f. Figure 3), the solution becomes virtually independent of ϵ .

Neglecting diffusion at the edges of the stream, the shape of a truncated Gaussian density profile is preserved as the stream propagates. The maximum mass flow that can survive magnetic stripping and proceed beyond position s on the horizontal stream is given by $\int_{(\frac{s}{a_n})^2 + (\frac{s}{a_z})^2 \leq 1} \rho u_{s0} \, dn \, dz$. Consistent with neglecting diffusion, we consider only the mass flow \dot{m} on those stream lines that have not yet coupled to the magnetosphere. This introduces a minimum over all previous stream coordinates s . This has a significant effect only for $\epsilon \lesssim 0.08$, for which stripping near L_1 occurs. Evaluation of the integral in elliptical coordinates and substitution of Equation (2), (3) and (6) results finally in

$$\begin{aligned} \dot{m}(s) &= \min_{s' \leq s} \left(1 - e^{-\sigma(s')} \right) = \\ &= 1 - \max_{s' \leq s} \left(\frac{\epsilon^2 B_0^2 u_{s0}}{2 \sqrt{\gamma \chi} (u_{s0}^2 \sin^2 \varpi + 2\epsilon^2)} \right). \end{aligned} \quad (9)$$

The symmetry of the integration region causes the first order error terms to cancel. The resulting stripping rate $\Lambda = -d\dot{m}/ds$ is then given by

$$\Lambda = \frac{d}{ds} \max_{s' \leq s} \left(\frac{\epsilon^2 B_0^2 u_{s0}}{2 \sqrt{\gamma \chi} (u_{s0}^2 \sin^2 \varpi + 2\epsilon^2)} \right), \quad (10)$$

wherein B_0 , u_{s0} , γ and χ are all regarded as functions of s .

At the L_1 -point we have a mass flow \dot{m} slightly below 1 since the magnetic pressure is very small in comparison with the gas pressure there but it is not vanishing totally. This is not a major inconsistency in our model since, as discussed above, our approximation of a dipole field is already very inaccurate in this region. However for sensible values of ϵ the stripping occurs mainly at large distances from the L_1 -point, where our approximation holds well (see Figure 3). The allowed mass flow \dot{m} is monotonically decreasing by construction of Equation (9), so un-physical negative stripping rates are ruled out. The above calculation did not account for blocking of the stripped matter by the dense core of the stream as proposed by Mukai (1988). Surface currents induced in the stream lead to a large local distortion of the threading field which then voids the stream; hence our model assumes that matter stripped of the back side is led around the stream by the distorted field lines.

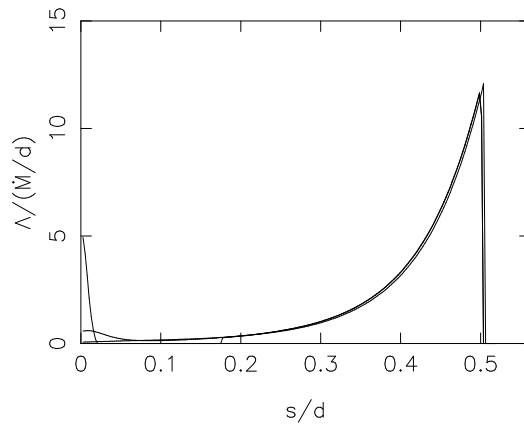


Figure 3. The stripping rate Λ according to Equation (10) for the HU Aqr geometry (see Table 1); ϵ takes the values 0.04, 0.12, and 0.36.

3 GEOMETRY OF THE ACCRETION CURTAIN

3.1 The threading process

Liebert & Stockman (1985) point out that the threading of matter onto the magnetic field involves a variety of physical processes, which are not yet fully understood (c.f. Cropper 1990, Warner 1995). However it seems clear that in accretion onto compact objects magnetic instabilities play the key role. Burnard et al. (1983) have shown that Kelvin-Helmholtz instabilities caused by a shear flow with inhomogeneous density distribution generate small drops which are easily captured by the magnetic field. It is also suggested that, even though the gas stream is highly supersonic, the negative density gradients additionally produce Rayleigh-Taylor instabilities. By these instabilities the stream is broken up into large diamagnetic blobs that, in contrast, are only slowly penetrated by the magnetic field. We assume here that the stripping is primarily driven by Kelvin-Helmholtz instabilities. In our model the droplets stripped from the surface follow abruptly the magnetic field lines and their kinetic energy from the motion perpendicular to the field is instantaneously thermalised. It turns out that the resulting rise in temperature allows the flow to become subsonic again.

3.2 The magnetic curtain

In the previous section we have modelled the rate at which material from the horizontal stream is captured by the magnetic field. The geometry of the threading region depends on the mass ratio Q and on the orientation of the magnetic dipole (ϑ_d, φ_d) relative to the canonical Cartesian system of the co-rotating frame. In polar coordinates (r, θ, ψ) aligned with the dipole we use the usual parameterisation of the field lines in azimuth ψ and equatorial radius r_m ; a dipole field line is then described as a function of the co-latitude θ by

$$\psi = \text{const}, \quad r = r_m \sin^2 \theta. \quad (11)$$

For an arbitrary threading point $(x, y, 0)$ on the horizontal stream we now consider the spherical triangle with the dipole axis, its projection onto the x - y plane, and the threading point as corners. The angle φ_c from the projected dipole axis to the threading point is given implicitly by

$$\tan(\varphi_d + \varphi_c) = \frac{-y}{1 - \mu - x}, \quad (12)$$

wherein the quadrant is provided by the standard sign convention for the denominator. Spherical trigonometry provides the coupling co-latitude θ_c and azimuth φ_c in dipole coordinates

$$\cos \theta_c = \cos \varphi_c \sin \theta_d, \quad \sin \psi = \frac{\sin \varphi_c}{\sin \theta_c}, \quad (13)$$

which is unique since in our case always $\theta_c \in [0, \pi[$ and $\psi \in [-\frac{\pi}{2}, \frac{\pi}{2}]$, it is also clear that always $|\sin \varphi_c| \leq |\sin \theta_c|$. The above set of equations seems to us slightly easier than the one given by Ferrario (1989), but nevertheless describes the same geometry. Equation (11) finally yields the equatorial radius of the threading field line

$$r_m = \frac{r_c}{\sin^2 \theta_c}. \quad (14)$$

We obtain the initial velocity with which the stripped material moves on the curtain from the purely kinematic argument that the component parallel to the field lines is conserved. For the dipole orientation in HU Aqr (see Table 1) it turns out that the material turns a rather sharp corner of $\varpi \approx 75^\circ$. If we use a mass specific Roche potential normalised with an additive constant such that $\Phi(L_1) = 0$ the dissipated energy per unity mass is given as $-\Phi_c \sin^2 \varpi$, where Φ_c is the potential at the coupling point. Towards the end of the horizontal stream the energy loss for an H-atom is nearly 1 keV. We assume for our model that the resulting rise in temperature is relaxed instantaneously to the isothermal equilibrium temperature characterised by the isothermal sound speed ϵ - in practice a different value of ϵ may apply to each field line in the curtain.

Continuity and momentum conservation for an isothermal flow inside a flux tube provide a differential equation for the velocity u along the field lines, given the magnetic field B and the Roche potential Φ

$$\frac{du}{u} \left(\frac{\epsilon^2}{u^2} - 1 \right) = \frac{\epsilon^2}{u^2} \frac{dB}{B} + \frac{1}{u^2} d\Phi; \quad (15)$$

Shortly after coupling the stream becomes highly supersonic again, hence pressure effects are negligible everywhere and we get by integration

$$u \approx \sqrt{2(\Phi_c \sin^2 \varpi - \Phi)}, \quad (16)$$

which is simply energy conservation for a free falling particle. In principle the field lines could lead so far uphill in the Roche potential that Equation (15) predicts the material to stagnate somewhere with zero velocity. For the HU Aqr geometry this case never occurs in our simulation.

Gliding down the field lines the material from the stream forms an essentially two-dimensional curtain. We now introduce a curtain coordinate system (c.f. Figure 4) which consists of the distance s of the coupling point from L_1 , the magnetic co-latitude θ , and the distance b perpendicular to the curtain. The coordinates are orthogonal at the coupling point and the curves of constant b are field lines.

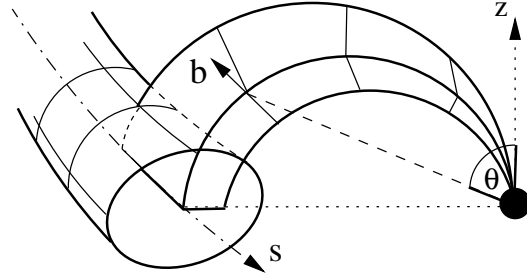


Figure 4. Sketch of the horizontal stream with a part of the accretion curtain, which illustrates the coordinates introduced in the text.

Since the curtain flow follows field lines, we can represent the density as

$$\rho = \sigma_c(s, \theta) f(\Delta^{-1}b), \quad (17)$$

where the typical width Δ of the curtain depends on s and θ . The convergence of field lines along the curtain flow can be expressed by the variation of the thickness of a flux tube perpendicular to the direction of motion. For the flux tube starting at stream coordinate s the distance dl to the adjacent field line starting at $s + ds$ is given by

$$\left(\frac{\partial l}{\partial s} \right)^2 = h_{r_m}^2 \left(\frac{\partial r_m}{\partial s} \right)^2 + h_\psi^2 \left(\frac{\partial \psi}{\partial s} \right)^2, \quad (18)$$

where the derivatives $(\partial r_m / \partial s)$ and $(\partial \psi / \partial s)$ are a direct consequence of Equation (12)-(14) with $x = x(s)$ and $y = y(s)$. The metric coefficients $h_{r_m}^2$ and h_ψ^2 are given by Equation (B6) and (B7) as functions of θ and r_m .

The mass flow transported on the flux tube defined by s and $s + ds$ is given by Λds (c.f. Equation (10)). As a consequence of continuity we have then

$$\sigma_c = \frac{\Lambda}{u} \left(\frac{\partial s}{\partial l} \right) = \frac{\Lambda}{u} \left[h_{r_m}^2 \left(\frac{\partial r_m}{\partial s} \right)^2 + h_\psi^2 \left(\frac{\partial \psi}{\partial s} \right)^2 \right]^{-\frac{1}{2}}; \quad (19)$$

at the coupling point we know from simple geometry that $(\partial l / \partial s)_0 = \sec \varpi$ holds. Since the flow is bound to a flux tube, we can write the typical width of the curtain as $\Delta^{-1} \propto B(\partial l / \partial s)$. A quite suitable choice for f could be a Gaussian profile with a dispersion Δ , for which at the coupling point $\Delta^2 = a_n a_z$ holds.

4 SIMULATION OF DOPPLER MAPS AND TRAILED SPECTRA

4.1 Companion star line emission

Our model assumes that the companion star exactly fills its Roche lobe, that the reprocessed radiation is proportional to the absorbed X-rays, and that the emission is diffuse according to the foreshortening given by Lambert's law, i.e. with a cosine dependency of the viewing angle. Isotropic re-emission has shown to provide a less accurate line profile. Thermal broadening at the bulk temperature causes a velocity dispersion $\epsilon \Omega d / c$, which is just above the numerical resolution of our spectral grid. The X-rays are assumed to

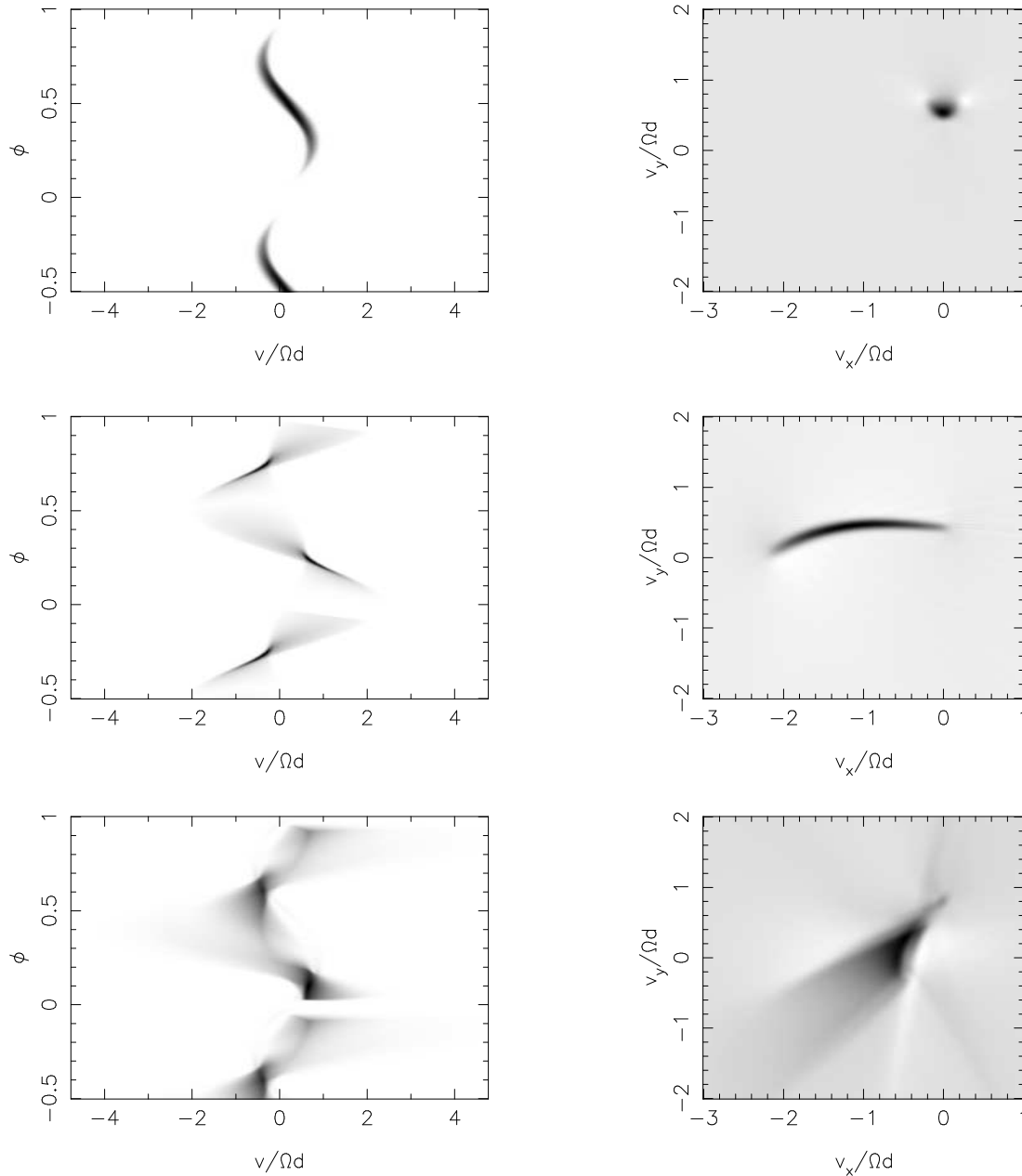


Figure 5. Model line emission from various parts of the system displayed as trailed spectra (first column) and in the Doppler tomograms (second column) calculated by a filtered back-projection. Rows: (a) companion Roche lobe, (b) horizontal steam, (c) accretion curtain. The gray-scale of each row is chosen separately. Model parameters as given in Table 1.

originate from a point source at the white dwarf’s centre. The involved error in the location of the X-ray source is of the order of the white dwarf radius R_{wd} , i.e. typically 1% of the orbital separation d .

The upper panel of Figure 5 shows the emission arising of the X-ray heated face of the secondary Roche lobe. To match the orientation of Doppler maps usual in the literature we invert the sign convention of the v_x and v_y axes with respect to the x and y coordinates, respectively. The numerical calculation makes use of the fact that obviously the secondary star is totally opaque to X-rays and to optical line emission. The resulting self-occultation of the Roche lobe

should provide a constraint on the orbital inclination, but the endpoints of the narrow emission line (NEL) eclipse are superimpose with emission from the stream. We therefore use the inclination determined for a given mass ratio from the eclipse width in the optical light curve. The K-velocity and the width of the secondary star emission feature can be used to estimate the relative Roche lobe size, and hence for the mass ratio. The maximum width of this feature is given as 2.45\AA by Schwope et al. (1997a), which unfortunately is not far from the spectral resolution (1.6\AA).

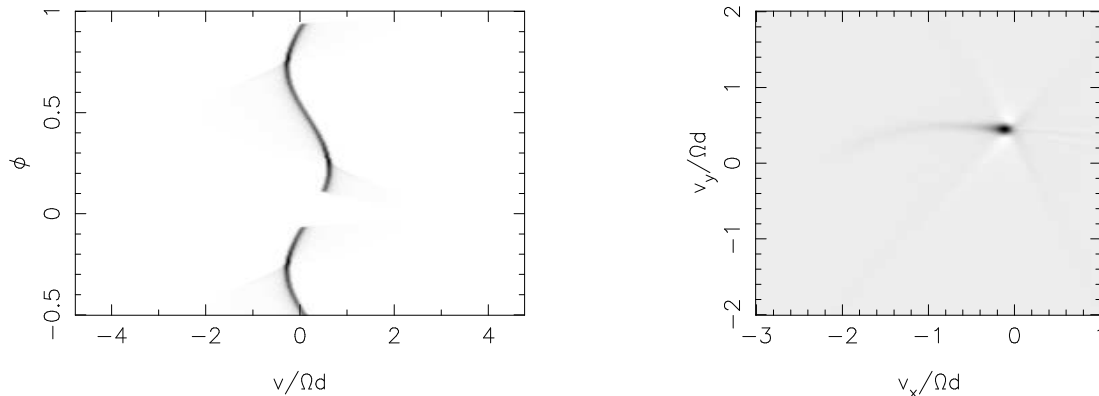


Figure 6. Synthetic trailed spectrum of reprocessed line emission from the secondary star in assumption of a fully transparent stream in X-rays and line. This is to be compared to the middle row of Figure 5. Doppler tomogram.

4.2 Emission of the horizontal stream

The horizontal stream emission is shown in the middle panel of Figure 4. Our model assumes that the horizontal stream is opaque to X-rays but transparent to the optical line photons. For phases smaller than approximately 0.55 we are viewing the irradiated side of the stream facing the X-ray source; in contrast, for phases larger than about 0.55 we are facing the un-irradiated side, however the observed emission in the HeII 4686Å line is just slightly lower by about 20% in the observations (c.f. Schwope 1997a). So the horizontal stream cannot be opaque for both the X-ray irradiation and the optical line emission. Simulated tomograms (see Figure 6) show that the stream cannot be fully transparent in both spectral regimes either. In that case the volume emissivity would be proportional to the square of the local density, which produces too much emission close to the L_1 -point. It has been observed that the Roche lobe is significantly shielded from the X-ray irradiation by the accretion curtain, which is even more dilute than the horizontal stream. So we suggest a horizontal stream opaque to the ionising radiation but nearly fully transparent in the HeII line so that we observe the irradiated front side even when viewing through the stream. The low line opacity needed seems plausible, given the large velocity gradients in the stream.

These arguments make it plausible that the line radiation mainly stems from the skin layers of the stream, which probably is surrounded by some kind of hot X-ray heated corona. If we assume that the radiation reprocessing involves the same physical process as on the companion Roche lobe, then comparison of the relative fluxes allows an estimate of the stream width, which is proportional to ϵ . Knowledge of ϵ in turn allows an estimate of the core temperature of the stream.

Gaussian fitting of the high velocity component (HVC) emission shows clearly a fading of the horizontal stream around phases 0 and 0.5 (gaps). This suggests a foreshortened optically thick emission. However the above argument gives evidence for an optically thin stream transparent to optical line photons. We therefore propose a thin X-ray heated

region that is optically thick and reprocesses most of the ionising radiation whereas the remainder of the stream is optically thin. The resulting spectra are shown in the middle panel of Figure 5. We do not expect information from the gaps to be of great importance for the parameter fitting because of the rather poor signal to noise ratio at these phases. However, compared to the observational data they occur at quite the right phase and velocity in our simulations. The rather narrow emission lines (knots) at $\varphi \approx 0.22$ and $\varphi \approx 0.72$ occur when the orientation of the stream to the line of sight is such that the intrinsic velocity plus the orbital speed are virtually constant over the length of the stream. In addition at $\varphi \approx 0$ occultation by the secondary star shields the stream from the observer. Whereas the amplitude and the phases of the maxima of the horizontal stream emission can be adjusted to the observational data by an appropriate choice of the model parameters, the line profile of the high velocity wings provides a test to the correctness of our stripping model.

4.3 Emission of the accretion curtain

The broad baseline component (BBC) emitted by the accretion curtain (see bottom panel of Figure 5) appears very dim in the modelled trailed spectra and in the Doppler tomograms since it is distributed over a large range of velocities. We assume the line emission is proportional to the intercepted X-rays. As for the horizontal stream the eclipse of the curtain is modelled with a spherical companion star of the effective Roche radius. The brightest part of the curtain is the stagnation region in which the material enters the curtain when it couples to the magnetosphere. Emission from the curtain partially covers up the gaps of the horizontal stream emission in the trailed spectrum of the middle row of Figure 7, in which the three components (Roche lobe, horizontal stream, and curtain) are merged.

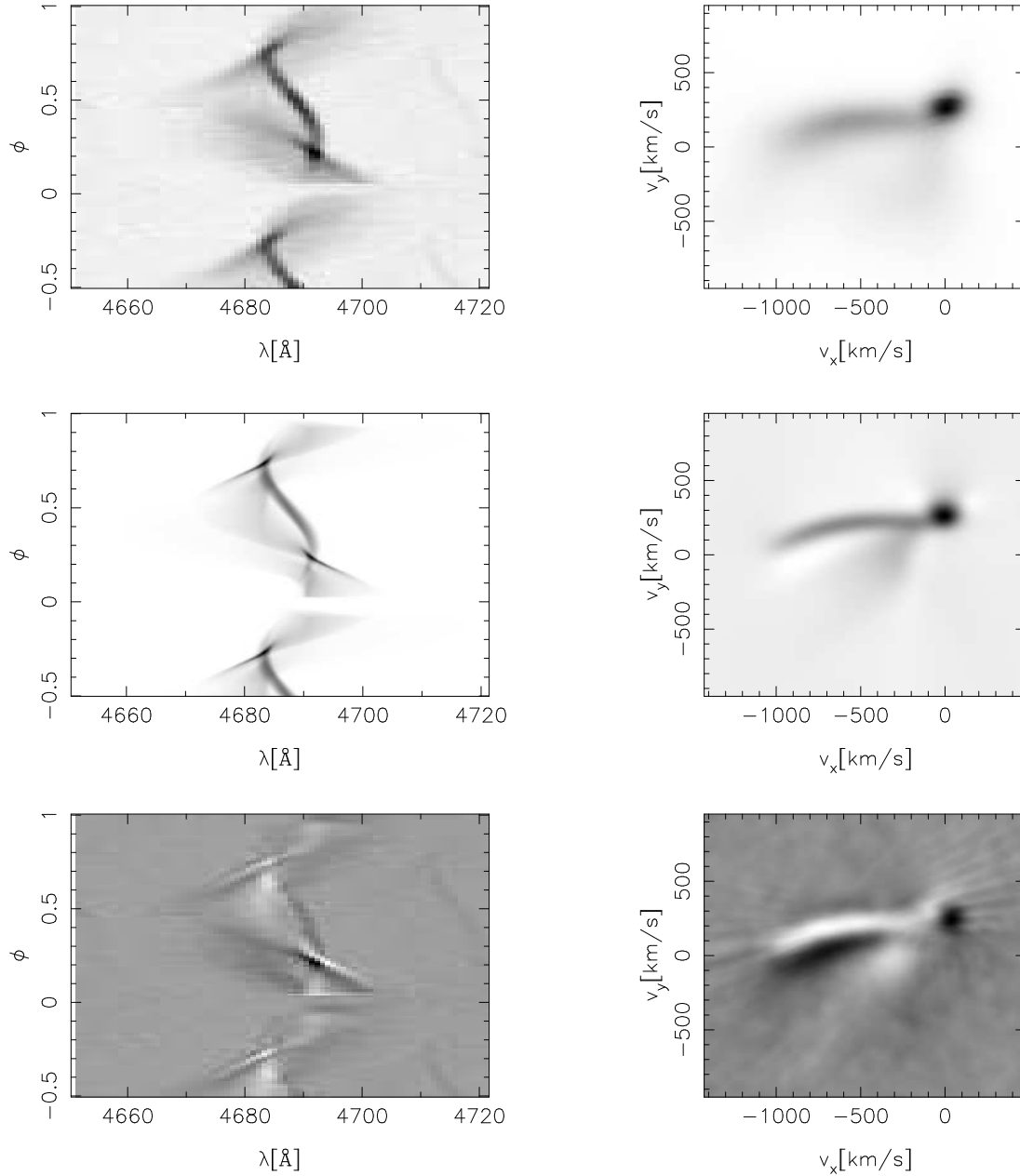


Figure 7. Comparison between the observational data of HU Aqr in He II 4686 (upper row) and the model folded with the spectral resolution (middle row), the residuals are shown in the bottom row. Displayed are the trailed spectra (l.h.s.) and back-projected Doppler tomograms (r.h.s.), apart from the top right panel where MEM tomography was used. Model parameters from Table 1.

5 TESTING THE MODEL

To adjust the 10 free parameters of the model, which are given in Table 1, we have performed a χ^2 -fit to the HU Aqr trailed spectra from August 1993, when the object was in its high accretion state. We focus on the 4686Å He II line which has the best signal to noise ratio and shows the sharpest features of all lines in the observed spectral range from 4180 Å to 5070 Å. Figure 7 compares the observational data and our fitted model, which was folded by the observational resolution. The fitting employed a simplex algorithm to adjust 8 parameters in order to minimise the χ^2 statistic for which we have used estimated standard deviations from a detector

noise model. The orbital period P is very well known from long-term light curves; also from the optical eclipse the orbital inclination i of the system is given as a function of the mass ratio. So we have not varied these parameters in the fit.

There are certain features in the spectra which constrain particular parameters. With the period and mass ratio fixed the orbital separation d scales the wavelength axis. The mass fraction μ governs the width and amplitude of the Roche lobe emission. These two parameters hence are predominantly determined by the NEL feature, but the curvature of the horizontal stream also effects these parameters.

Table 1. Model parameters obtained from χ^2 -fitting; these are used for the figures shown in this article. The quantities where no error is given have not been varied in the χ^2 -fit.

parameter	symbol	value	error
orbital period	P	0. ^d 086820446	–
orbital inclination	i	84. ^o 0	–
orbital separation	d	$5.663 \cdot 10^{10}$ cm	$5.6 \cdot 10^8$ cm
mass fraction	μ	0.7950	0.0027
magn. momentum	$\epsilon \mathcal{M}$	0.0771	0.0035
dipole azimuth	φ_d	37. ^o 8	1. ^o 6
dipole co-latitude	ϑ_d	12. ^o 4	0. ^o 3
sound speed	ϵ	0.0355	0.0016
rest wavelength	λ_0	4685.7Å	0.1Å
rel. curtain intens.	I_c	0.0154	0.0023

The resulting Q ratio of 3.9 lies in between the two values obtained by Schwöpe (1997a) from either of these features separately. With d and μ fixed, the length of the horizontal stream is determined by the magnetic dipole parameters \mathcal{M} , φ_d and ϑ_d . However the magnetic field strength varies strongly with the distance from the white dwarf and only weakly with the dipole orientation, thus the latter cannot be well constrained alone from a fit to the trailed spectrogram. Therefore we employ the knowledge of the accretion spot position ($\varphi_s = 40^\circ$, $\vartheta_s = 26^\circ$), which is given by Schwöpe et al. (1997a), based on the X-ray bright phase and cyclotron harmonics. We have used the mass radius relation for white dwarfs given by Pringle (1975) to constrain our variation of φ_d and ϑ_d to those values that are in agreement with the observed accretion spot. The sound speed ϵ is a measure of the bulk temperature, which scales the geometrical width of the horizontal stream. Thus its total brightness provides the information to which ϵ is fitted. The model also contains the relative brightness I_c of the curtain and the rest wavelength λ_0 as free parameters.

The error estimates given in Table 1 have been obtained by bootstrapping the original observation. On each pixel a random signal was added with the detector noise as standard deviation. We have repeated the χ^2 -fit starting with the same initial values for 20 different samples. The errors in Table 1 are 1σ intervals of the fitted parameters and consequently are only a measure of the uncertainty due to the noise in the data. They certainly do not account for systematic discrepancies of the model from reality (see Section 6).

From the fitted model parameters we are able to derive a couple of physical parameters of the *HU Aqr* system. With the observed magnetic field at the accretion spot of 35 MG we are able to scale our intrinsic units from Equation (1) to physical units. This enables us to determine the total mass accretion rate as $\dot{M} = 2.9 \times 10^{-10} M_\odot/\text{yr} (B/35\text{MG})^2 (\epsilon/0.0355)^2$. This value depends strongly on our assumption of identical effectivity of radiation reprocessing on the companion star surface and the horizontal stream. Here also the choice of the stripping condition and the assumption of a quasi-steady flow are very essential. Nevertheless the derived \dot{M} is not extremely far from $\dot{M} \approx 0.5 \times 10^{-10} M_\odot/\text{yr}$ estimated from the total luminosity of an average CV just below the period gap (Patterson 1984). The accretion rate in the model is lowered by a factor of 4 when either the radiation reprocessing in the

Table 2. Some physical quantities of *HU Aqr* as derived from the model parameters given in Table 1.

quantity	symbol	value
mass ratio	Q	3.9
dip angle	ϕ_{dip}	-0.117
primary mass	M_{wd}	$0.75 M_\odot$
secondary mass	M_{rd}	$0.19 M_\odot$
white dwarf radius	R_{wd}	$7.3 \cdot 10^8$ cm
secondary Roche radius	R_{rd}	$1.5 \cdot 10^{10}$ cm
bulk temperature	T	$17 \cdot 10^3$ K
total mass flow	\dot{M}	$2.9 \cdot 10^{-10} M_\odot/\text{yr}$
coupling density	n	$7.6 \cdot 10^{-11} \text{g}/\text{cm}^3$

horizontal stream is twice as effective as on the Roche lobe, or if matter coupling to the magnetosphere needs a magnetic field twice as large as assumed.

In the optical light curve a pre-eclipse dip centred at phase $\phi = -0.118$ has been observed; it has a symmetric distribution that can well be approximated by a Gaussian profile with a dispersion of 0.015. Our model cannot account for this dispersion, which is presumably a consequence of the matter being broken up into blobs of different sizes, hence the threading points vary over a range of locations. The good agreement of the modelled turn-off point at phase $\phi = -0.117$ shows that the horizontal stream is free falling in a good approximation. So the geometrical location of the coupling region and the fitted location in velocity space coincide.

The model also gives strong evidence that the companion star is on the main sequence. The radius of a main sequence star with a mass of $0.19 M_\odot$ is given by Neece (1984) as $0.23 R_\odot$ which agrees very well with the effective radius of the Roche lobe provided by Eggleton (1983) which comes out to be $0.22 R_\odot$ for our values of μ and d . We do not have to assume a mass radius relation for this result.

At the coupling point we have a mass density of $7.6 \times 10^{-11} \text{g}/\text{cm}^3$ or, for a pure hydrogen gas, a number density of $n = 4.2 \times 10^{16} \text{cm}^{-3}$, which results in a Debye length of $\lambda_d = 4.1 \times 10^{-3} \text{cm}$. Hence we have an ideal plasma with a plasma parameter $\Gamma := 1/(n\lambda_d^3) = 3 \times 10^{-10}$.

6 DISCUSSION

In the comparison between our model and the observational data of Figure 7 five details differ significantly: (1) At the location of the Roche lobe feature the residual tomogram shows a dark spot at positive v_x and a bright region towards negative v_x . This is a consequence of the missing shielding of X-ray flux by the curtain in our model. (2) The horizontal stream in the observation is clearly shifted in direction of smaller v_y . This is not a tomographic artefact as it is also clear from the residuals in the trailed spectrum near the knot at $\phi = 0.22$ that the simulation and observation are shifted against each other. The reason for this might be a magnetic drag force that acts transversely on the horizontal stream before the matter is totally coupled to the field. (3) The curtain emission seems to be too faint at low velocities in the model spectra and also ranges out to too high velocities.

Also the curtain is located at lower v_y in the model than in the tomogram of the observed data. This could be explained either by a reduction of radiation reprocessing when the curtain gets closer to the white dwarf, or by the importance of pressure effects when the curtain is funneled towards the accretion spot, or as well by a distortion of the dipole geometry. There also is a noticeable difference in the shape of the eclipse, so it might be suggested that the reason lies in the geometry of the curtain flow. (4) The observed tomogram shows faint but significant emission in the region roughly between $(v_x, v_y) = (-900, 0)$ to $(-1200, -600)$, which cannot be explained in our model. A plausible speculation on the origin of this emission could be larger blobs in the horizontal stream that are sufficiently massive to survive the stripping process but feel a strong drag force by the magnetic field that forces them to leave the ballistic trajectory. (5) Even though folded with the observational resolution the widths of all modelled stream features are too small in both the trailed spectra and the Doppler tomograms. This could be caused by an underestimate of the observational resolution, or an intrinsic line broadening. Thermal broadening of the bulk temperature is already included in the model, the gas is much too dilute for pressure broadening, and the field strength is much too low for a noticeable Zeeman effect. However the layer in which the radiation reprocessing occurs may be heated far above the bulk temperature. This hot corona-like gas around the stream could be the source of the large observed line width. Also broadening by turbulent gas motion might be important.

We have developed a predictive model for the stripping of the accretion stream and the line emission in AM Her stars in general and applied it to spectral observations of the eclipsing polar HU Aqr in its high accretion state. The main observed features, including the length of the horizontal stream and the main emission line components, are well reproduced by our model. A χ^2 -fit of synthesised to observed trailed spectrograms has uncovered a number of physical parameters of the binary system (mass flow rate, stream temperature, stream density, orientation of the magnetic field, mass ratio etc.). The detailed comparison between observation and simulation (c.f. Figure 7) shows some systematic deviations which may be overcome by further improvements of the model. A possible cure for the above problems could be a numerical calculation of the field distortion in presence of a highly conducting plasma and a more detailed investigation on the flow instabilities. However on account of the enormous Reynolds numbers of the flow a fully self-consistent numerical model seems not feasible to us. A further improvement for the model would be a more precise calculation of the radiation reprocessing rather than just assuming limiting cases for the opacity, especially the velocity gradients in the stream could significantly alter the characteristics of the line radiation. However the overall agreement between observational data and the proposed model based on rather simplified physics seems remarkably good to us.

ACKNOWLEDGEMENTS

The authors would like to thank Danny Steeghs for providing a MEM tomogram of HU Aqr, and Rick Hessman, Thomas Neukirch, Moira Jardine and Miguel Ferreira for

very informative discussions. We gratefully acknowledge the Cormack Bequest Scholarship of the Royal Society of Edinburgh. Without its help and the hospitality of the AIP in Potsdam this project could not have been completed. This work has also been supported in part by the Deutsches Zentrum für Luft- und Raumfahrt (DLR, former DARA) under grant 50 OR 9403 5.

REFERENCES

- Burnard, D.J., Lea, S.M., Arons, J., 1983, ApJ 266, 175
 Cropper, M., 1986, MNRAS 222, 853
 Cropper, M., 1990, Sp. Sci. Rev. 54, 195
 Eggleton, P.P., 1983, ApJ 268, 368
 Ferrario, L., Wickramasinghe, D.T., Tuohy, I.R., 1989, ApJ 341, 327
 Glenn, J., Howell, S.B., Schmidt G.D., et al., 1994, ApJ 424, 967
 Hakala, P.J., Watson, M.G., Vilhu, O., et al., 1993, MNRAS 263, 61
 Hakala, P.J., 1995, A&A 296, 164
 Kevorkian, J., Cole, J.D., 1980, Perturbation Methods in Applied Mathematics, Berlin (Springer)
 Liebert, J., Stockman, H.S., 1985, in *Cataclysmic variables and low-mass X-ray binaries*, D.Q. Lamb and J. Patterson (eds.), Reidel, p. 151
 Lubow, S.H., Shu, F.H., 1975, ApJ 198, 383
 Lubow, S.H., Shu, F.H., 1976, ApJ 207, L53
 Mukai, K., 1988, MNRAS 232, 175
 Neece, G.D., 1984, ApJ 277, 738
 Patterson, J., 1984, ApJS 54, 443
 Pringle, J.E., 1975, MNRAS 172, 493
 Schneider, D.P., Young, P., 1980, ApJ 240, 871
 Schwartz, R.D., Dawkins, D., Findley, D., Chen, D., 1995, PASP 107, 667
 Schwope, A.D., Thomas, H.-C., Beuermann, K., 1993, A&A 271, L25
 Schwope, A.D., Mantel, K.-H., Horne, K.D., 1997a, A&A 319, 894
 Schwope, A.D., Beuermann, K., Buckley, D.A.H., et al., 1997b, Proc. 13th North American Workshop on CVs, Howell, S.B., et al. (eds.), ASP. Conf. Ser., in press
 Warner, B., 1995, Cataclysmic Variable Stars, Cambridge University Press

APPENDIX A: POWER SERIES FOR THE HORIZONTAL STREAM AT L_1

Vertical scale

In their classical paper on gas dynamics in semi-detached binaries Lubow & Shu (1975) assume that thermal equilibrium prevails in z -direction. In a later publication (1976) they give also a closed set of differential equations for the vertical structure of the stream:

$$u_{s0} \frac{d\chi}{ds} + 2\nu\chi = 0 \quad (\text{A1})$$

$$u_{s0} \frac{d\nu}{ds} + \nu^2 - \chi + \left(\frac{\partial^2 \Phi}{\partial z^2} \right)_0 = 0 \quad (\text{A2})$$

$$\chi(0) = A, \quad \nu(0) = 0 \quad (\text{A3})$$

Therein is $1/\sqrt{\chi}$ the dispersion of the vertical Gaussian, $\nu = \frac{\partial u_z}{\partial z}$ the divergence of the z -velocity and $\left(\frac{\partial^2 \Phi}{\partial z^2} \right)_0$ the

second derivative of the Roche potential taken at the stream centre.

L_1 is a singular point of these equations since energy conservation provides $u_{s0} = \lambda_1 s + O(s^2)$ and hence u_{s0} is vanishing at initial point $s = 0$. The similarity to Euler's equation suggests the 'Ansatz' as a fractional power series

$$\chi = A + \sum_{k=0}^{\infty} C_k s^{k+c}, \quad \nu = \sum_{k=0}^{\infty} N_k s^{k+b} \quad (\text{A4})$$

for some $b > 0$, $c > 0$ and sets $\{C_k\}_k$ and $\{N_k\}_k$ with $C_0 \neq 0$ and $N_0 \neq 0$, which provides uniqueness of the solution. After substitution and use of Cauchy's theorem the s^b -term in the χ -equation and the s^1 -term in the χ -equation provide $b = c = 1$, using the non-vanishing of C_0 and N_0 . This proves that the solution we are looking for is even analytical at L_1 , which has not been obvious a priori.

Knowing c and b we can compare the terms in s^k and obtain to first order

$$\chi = A + \frac{2A\Phi_{zzs}}{\lambda_1^2 + 2A} s + O(s^2) \quad (\text{A5})$$

$$\nu = \frac{\lambda_1\Phi_{zzs}}{\lambda_1^2 + 2A} s + O(s^2) \quad (\text{A6})$$

where, with the white dwarf mass fraction μ , we have been using the definitions

$$A := \frac{\mu}{|x_{L_1} - 1 + \mu|^3} + \frac{1 - \mu}{|x_{L_1} + \mu|^3} \quad (\text{A7})$$

$$\lambda_1^2 := \frac{1}{2} \left(A - 2 + \sqrt{9A^2 - 8A} \right) \quad (\text{A8})$$

$$\Phi_{zzs} := \left(\frac{\partial^3 \Phi}{\partial^2 z \partial s} \right)_{L_1} \quad (\text{A9})$$

Horizontal scale

Let $1/\sqrt{\gamma}$ be the horizontal dispersion of the Gaussian density profile of the stream, $\beta = \frac{\partial u_n}{\partial n}$ the divergence of the n -velocity and $K = 1/R$ the curvature of the ballistic trajectory. Then the differential equations for the horizontal stream width are, as derived by Lubow & Shu (1975):

$$u_{s0} \frac{d\gamma}{ds} + 2\beta\gamma = 0 \quad (\text{A10})$$

$$u_{s0} \frac{d\beta}{ds} + \beta^2 - \gamma = (2 - 3Ku_{s0})Ku_{s0} - \left(\frac{\partial^2 \Phi}{\partial n^2} \right)_0 - 4 \quad (\text{A11})$$

$$\beta(0) = 0, \quad \gamma(0) = \lambda_1^2 - A + 3 =: \lambda_3^2, \quad (\text{A12})$$

where we have already substituted the analytical integrals found by Lubow & Shu. The singularity of these equations is of the same kind as for the vertical structure, hence we are claiming again that γ and β can be written as fractional power series. A somewhat similar but more extensive algebra shows then that the solution of the horizontal equations is also analytical. As first order solution we obtain

$$\gamma = \lambda_3^2 + \frac{(12K_0\lambda_1 - \Phi_{nns})\lambda_3^2}{2\lambda_3^2 + \lambda_1^2} s + O(s^2) \quad (\text{A13})$$

$$\beta = \frac{(6\lambda_1 - \Phi_{nns})\lambda_1}{2\lambda_3^2 + \lambda_1^2} s + O(s^2), \quad (\text{A14})$$

where K_0 is the curvature at the L_1 -point and

$$\lambda_3^2 := \lambda_1^2 - A + 2 \quad (\text{A15})$$

$$\Phi_{nns} := \left(\frac{\partial^3 \Phi}{\partial^2 n \partial s} \right)_{L_1} \quad (\text{A16})$$

APPENDIX B: MAGNETIC FOCUSING IN THE CURTAIN PLANE

We now consider the magnetic focusing in the curtain plane. Be P a fixed point with co-latitude θ on an arbitrary field line (r_m, ψ) . On a neighbouring field line $(r_m + dr_m, \psi + d\psi)$ a point Q with the co-latitude $\theta + d\theta$ has a distance dl from P which is to first order in the locally Euclidean metric

$$(dl)^2 = (dr)^2 + (rd\theta)^2 + (r \sin \theta d\psi)^2 \quad (\text{B1})$$

where

$$r = r_m \sin^2 \theta \quad (\text{B2})$$

$$\begin{aligned} dr &= (r_m + dr_m) \sin^2(\theta + d\theta) - r = \\ &= (2r_m \sin \theta \cos \theta) d\theta + (\sin^2 \theta) dr_m \end{aligned} \quad (\text{B3})$$

The condition for a critical point is given by $\frac{\partial}{\partial(d\theta)}(dl)^2 = 0$ and yields as a unique solution

$$d\theta = -2 \frac{\cos \theta \sin \theta}{r_m(1 + 3 \cos^2 \theta)} dr_m, \quad (\text{B4})$$

which, if $\theta > -d\theta$, actually provides by substitution into Equation (B1) the real minimum distance dl between P and any point $Q(\theta + d\theta)$ on a neighbouring field line:

$$(dl)^2 = h_{r_m}^2 (dr_m)^2 + h_{\psi}^2 (d\psi)^2 \quad (\text{B5})$$

$$h_{r_m}^2 := \frac{1 - \cos^6 \theta + 3 \cos^4 \theta - 3 \cos^2 \theta}{1 + 3 \cos^2 \theta} \quad (\text{B6})$$

$$h_{\psi}^2 := \frac{r_m \sin^2 \theta (1 + \cos^2 \theta)}{1 + 3 \cos^2 \theta} \quad (\text{B7})$$